Contents:

SUPPLEMENTARY MATERIALS/METHODS

***In vitro* GSK-3β kinase activity assay**. Full length, human GSK-3β (NM_002093) with an N-terminal GST tag was obtained from BPS Biosciences. Glycogen synthase peptide substrate (GSP-2; Tyr-Arg-Arg-Ala-Ala-Val-Pro-Pro-Ser-Pro-Ser-Leu-Ser-Arg-His-Ser-Ser-Pro-His-Gln-Ser(PO_3H_2)-Glu-Asp-Glu-Glu-Glu; purity >95%) was purchased from American Peptide International. 20 μl total volume of CABPE mix (25 mM Tris, 10 mM $MgCl_2$, 5 mM DTT, 0.1 mg/ml BSA, 0.2 U/ml Heparin, 4.8 μM of GSP-2 peptide substrate, 20 ng/well GSK-3β) was added to each well of a 384-well plate, and compounds of various concentrations were pin-transferred (100 nl) from stock compound plates to each well. 10 μl ATP (3 μM in CABPE mix without substrate or kinase) was then added to each well to reach a final ATP concentration of 1 μM. The reaction mix was incubated for 90 minutes at room temperature, and 30 μl Kinase-Glo

(Promega) was added to each well and incubated for additional 40 minutes before firefly luminescence signals were read on Envision (Perkin Elmer).

Pharmacokinetics study. Blood samples were collected by retro-orbital puncture into tubes containing sodium heparin anticoagulant at pre-dose and 5 min, 15 min, 30 min, 1 hr, 2 hr, 4 hr, 6hr, 8 hr, and 24 hours post-dose. Immediately after blood collection, mice were sacrificed by cervical dislocation and brain samples harvested and rinsed with saline. Analyses of samples were conducted by MPI (Preclinical Research LLC, Shanghai). Concentrations of CHIR99021 in plasma and brain samples were determined using a high performance liquid chromatography/mass spectrometry (HPLC: 1100 series (Agilent Technologies Inc), MS: API3000 (AB Inc, Canada)). The data acquisition and control system were created using Analyst 1.4 software from ABI Inc.

Histology and immunohistochemistry. Mice receiving intracerebroventricular infusions were cervically dislocated, brains removed and stored in 10% formalin until sectioning. Coronal sections (60 micron) spanning the cannula tract were processed on a cryostat and injection sites were verified by light microscope. Mice receiving HSV viral injections were perfused transcardially with ice-cold PBS followed by 4% paraformaldehyde. Brains were removed and stored in 4% paraformaldehyde, and soaked in 30% sucrose 4 days prior to sectioning. Coronal sections (30 microns thick) spanning the cannula tract were processed. Successful viral delivery in mice receiving HSV–β-gal was analyzed by immunocytochemical detection of β–galactosidase expression. To quantify AKT overexpression, sections were blocked in 10% goat serum in PBST (PBS with 0.1%Triton) and incubated overnight in anti-AKT primary antibody in the same buffer. Sections were subsequently incubated with a secondary antibody (Vector Laboratories (BA-1000, 1:1000, 5% goat serum in PBST). Immunoreactive cells

were visualized with DAB peroxidase substrate (Vector Laboratories SK-4100), imaged by light microscopy, and manually counted in three sections at 20x magnification per animal at the same approximate position relative to bregma according to lateral ventricle and anterior commissure landmarks. Only mice with correct placements were included in analyses.

Surgery. Mice were anesthetized with ketamine/xylazine (150 mg/kg and 10 mg/kg respectively; 5 ml/kg injection vol.). Using a stereotaxic apparatus, mice receiving intracerebroventricular infusions were implanted with stainless steel guide cannula with inserted dummy cannula (Plastics One) directed toward dorsal third ventricle (-0.5 mm posterior to Bregma, ± 0.0 lateral to midline, and -3.0 ventral to the skull surface). Mice recovered for least 5 days prior to testing and were gently restrained during infusions when dummy cannula were replaced with injection cannula connected to a 10 µl Hamilton syringe (Plastics One) through tubing. Infusions were controlled by a microinfusion pump (KD Scientific). Mice receiving intrastriatal or intracerebroventricular injections were anesthetized as described above. Using a stereotaxic apparatus, a 10 µl Hamilton syringe (Plastics One) was targeted bilaterally toward the striatum (+ 1.1mm anterior to Bregma, ± 1.3mm lateral to midline, -4.5mm ventral to the skull surface) or towards the third ventricle (- 0.5 mm posterior to Bregma, ± 0.0 mm lateral to midline, -3.0 mm ventral to the skull surface). For HSV injection, 0.5 µl of virus was infused over 2.5 minutes with an additional 2.5 minutes to ensure the virus fully absorbed into the tissue before syringe was slowly removed. Mice were given one day to recover prior to the first day of behavior testing due to maximal expression of HSV-AKT1 occurring 24-48 hours after administration and lasting only 7 days (Krishnan et al., 2008).

Immunoprecipitations. For each immunoprecipitation experiment, one whole mouse striatum was dissected on ice and placed directly in ice-cold 300 ul lysis buffer (10 mM Tris-HCL (pH 7.4), 1.0% Triton X-100) containing Roche complete protease inhibitor cocktail and varying concentrations of LiCl (0, 1 or 10 mM). The tissue was homogenized and then centrifuged for 15 min at 15,000xg at 4°C. Equal amounts of supernatant proteins were incubated in a volume of 200 ul with 30 ul immobilized anti-AKT antibody (#3653, Cell Signaling Technology), rotating overnight at 4°C. Immunoprecipitates were washed five times with Kudos buffer in the presence of 0.5% Triton, resuspended in 1X Laemmli loading buffer (Bio-Rad) and incubated at 42°C for 15 min before subjecting to Western blot analysis.

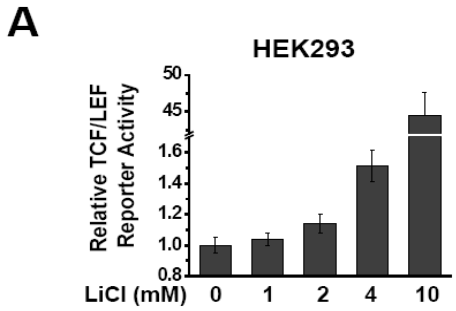

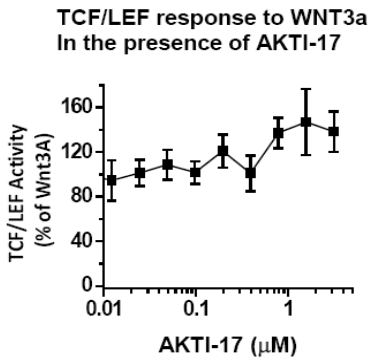

Supplemental Figure S1. (A) Lithium dose-dependently stimulates TCF/LEF reporter activity in HEK293 cells. HEK293 cells were treated with LiCl (0, 1, 2, 4, 10 mM) overnight, TCF/LEF mediated luciferase activity was measured by Dual-Glo (Promega), and normalized to Renilla luciferase activity under the control of ubiquitous EF1α promoter. TCF/LEF reporter activity is shown as the fold change relative to the control NaCl treatments. Data represents the average of at least three independent experiments. For all results, data are mean ± SEM. **(B) AKT1-17 does not inhibit the TCF/LEF activity induced by Wnt3a.** HEK293 cells were treated with AKTI-17 (0.001 - 5 μM) overnight in the presence of Wnt3a conditioned medium. Percent (%) TCF/LEF activity relative to the control Wnt3a response (AKTI-17 absent) is plotted against the concentrations of AKTI-17.

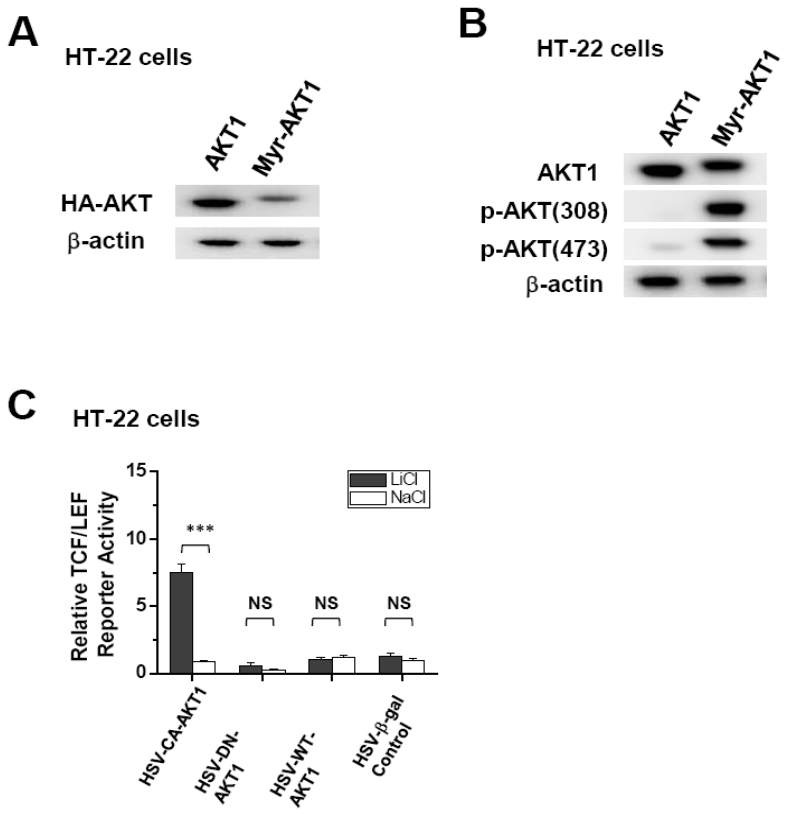

Supplemental Figure S2. Confirmation of exogenous AKT expression. (A) Exogenous WT-AKT1 and Myr-AKT1 were tagged by an HA epitope, and their expression in HT-22 cells were confirmed by Western blotting using an antibody against HA epitope. **(B)** Transfection of Myr-AKT plasmid resulted in the activating phosphorylation at both Thr308 and Ser473 residues. Antibodies against p-AKT(308), p-AKT(473) were used, and expression was normalized to a β-actin. **(C)** HT-22 cells were infected with Herpes Simplex viruses (~1 x 10^5 infection particles per ml) expressing constitutively active myristoylated AKT1 (HSV-CA-AKT), wild-type AKT1 (HSV-WT-AKT1), dominant negative AKT1 (HSV-DN-AKT1), or β-galactosidase (HSV-β-gal), and treated with LiCl or NaCl overnight. TCF/LEF activity is shown relative to the control condition (HSV-β-gal and NaCl treatment).

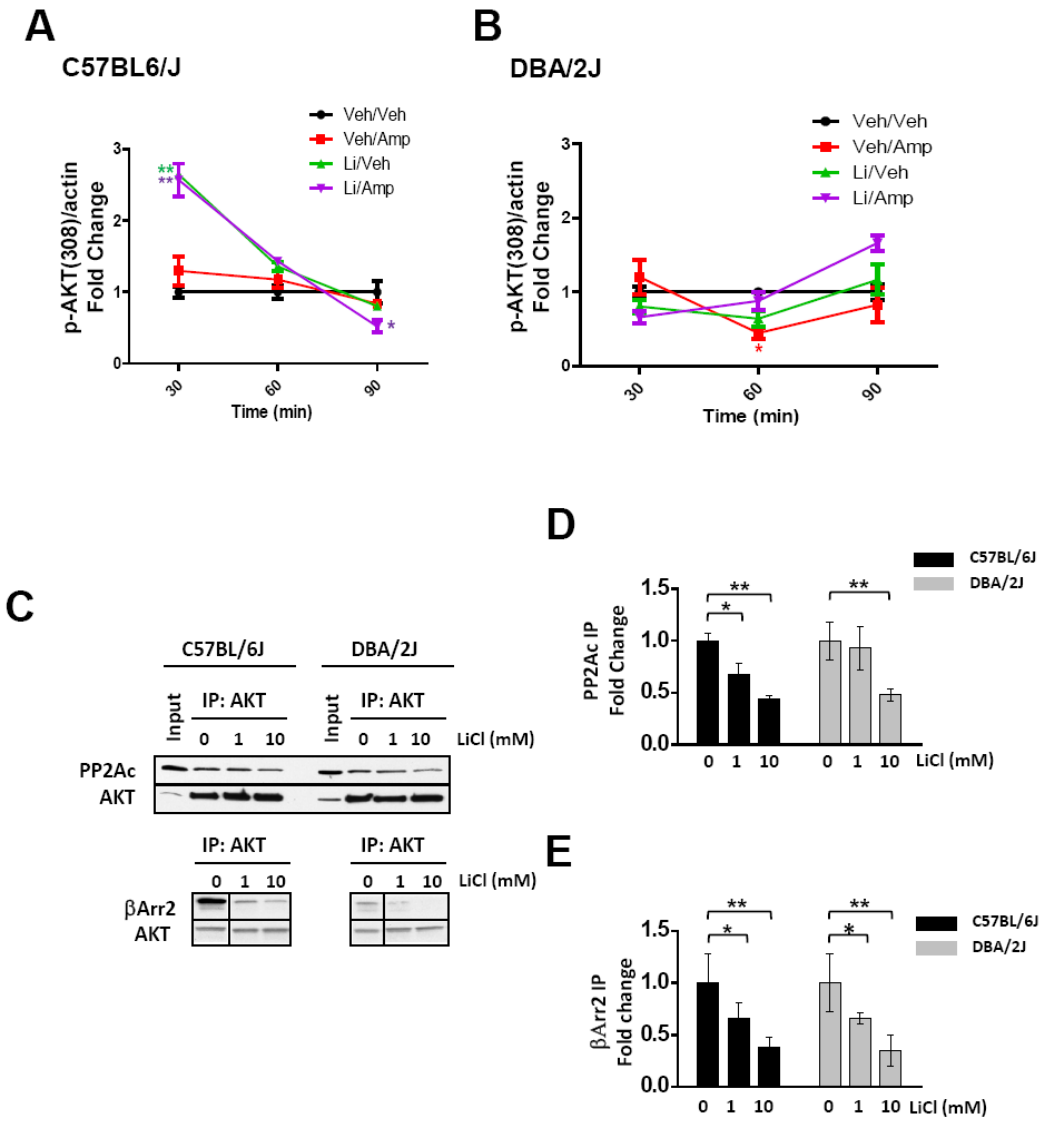

Supplemental Figure S3. Level of striatal pAKT(308) in C57BL/6J and DBA/2J mice induced by lithium treatment at 30, 60 and 90 minutes after amphetamine challenge. (**A**) C57BL/6J and (**B**) DBA/2J mice were pre-treated with vehicle or LiCl (85 mg/kg, i.p.) 60 minutes prior to vehicle or *d*-amphetamine challenge (3.5 mg/kg, i.p.), following the same administration scheme as behavioral studies. The striatal tissues were then harvested at 30, 60 or 90 minutes post-injection of amphetamine (or vehicle), and the protein extract analyzed by Western blot. Expression of p-AKT(308) was

normalized to a β-actin loading control, and fold change in p-AKT(308) compared to vehicle treatment in each mouse strain. Data represent the average of four animals in each treatment group (n=4). Statistics are based on one-way ANOVA for each time point. For C57BL/6J, $F_{treatment\text{-}30}$ (3,16) = 19.7, p = 0.0009; $F_{treatment\text{-}60}$ (3,16) = 2.6, p = 0.14; $F_{treatment\text{-}90}$ (3,16) = 9.0, p = 0.0061. For DBA/2J, $F_{treatment\text{-}30}$ (3,16) = 3.6, p = 0.75; $F_{treatment\text{-}60}$ (3,16) = 5.5, p = 0.024; $F_{treatment\text{-}90}$ (3,16) = 4.1, p = 0.059. Data are mean ± SEM. * $p < 0.05$ and ** $p < 0.01$ compared to vehicle-treated mice. **(C, D, E)** AKT was immunoprecipitated from C57BL/6J and DBA/2J striatal tissues and Western blotting was performed to measure the amount associated with βArr2 and the catalytic subunit of PP2A. Striatal tissue samples were prepared from naïve mice and incubated with beads covalently conjugated with an antibody against AKT in the absence or presence of lithium (0, 1 and 10 mM). **(C)** Representative Western blots of PP2A catalytic subunit and βArr2 co-immunoprecipitated with AKT. **(D, E)**. Densitometric analysis of the amount of βArr2 and PP2A proteins co-immunoprecipitated with AKT. Expression of βArr2 and PP2A catalytic subunit was normalized to AKT loading control from the same sample, and protein levels of samples in the presence of lithium compared to samples in the absence of lithium within each strain. For all results, data are mean ± SEM and represent two independent experiments.

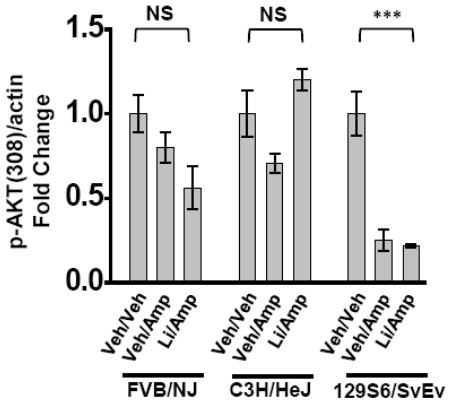

Supplemental Figure S4. Level of striatal pAKT(308) in FVB/NJ, C3H/HeJ, or 129S6/SvEv mouse strains by lithium treatment. Mice were pre-treated with vehicle or LiCl (85 mg/kg, i.p.) 60 minutes prior to vehicle or *d*-amphetamine challenge (3.5 mg/kg, i.p.), following the same administration scheme as behavioral studies. Striatal tissues were then harvested at 30 minutes post-injection of amphetamine (or vehicle), and the protein extract analyzed by Western blot. Densitometric Western blot analysis of relative amounts of p-AKT(308) in protein extract prepared from striatum are shown. Expression of p-AKT(308) was normalized to a β-actin loading control, and fold change in p-AKT(Thr308) compared to vehicle treatment in each mouse strain was shown. Data represent the average of four animals in each treatment group (n=4). Two-way ANOVA, F_{strain} (2,36) = 28.9, p = 0.001; $F_{treatment}$(2,36) = 25.8, p = 0.0001, $F_{interaction}$(2,36) = 16.9, p = 0.001. For all results, data are mean ± SEM. * p< 0.05 and ** p< 0.01 compared vehicle-treated mice; NS, p> 0.05.

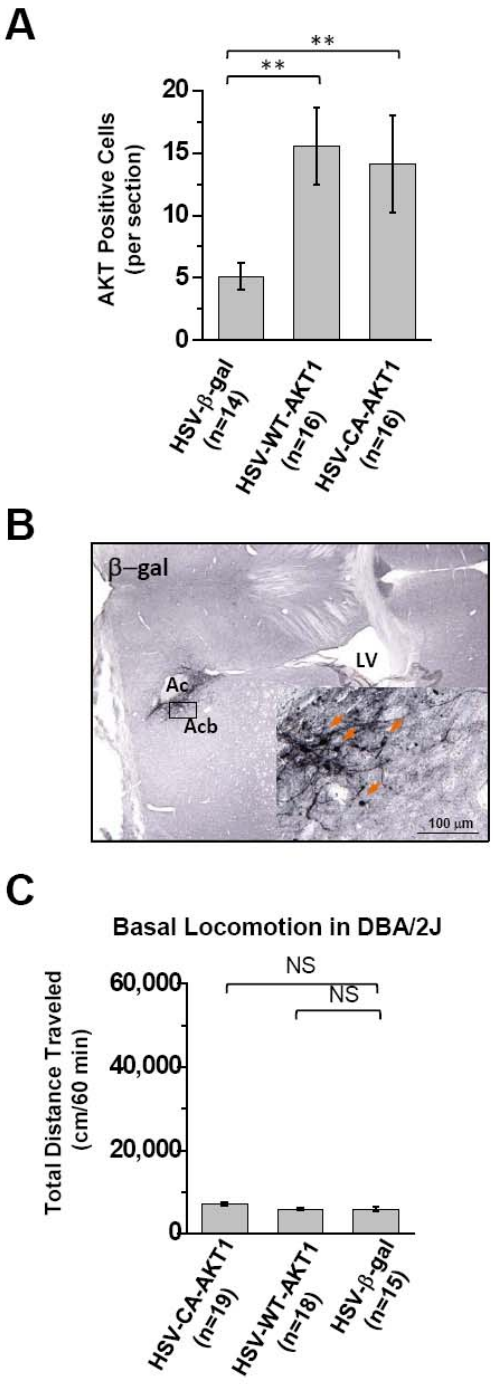

Supplemental Figure S5. (A) Immunohistological analysis of HSV mediated gene expression in striatum. Immunohistological analysis of AKT over-expression in the

striatum of DBA/2J mice. 30 micron sections were taken from representative mice from each of the three treatment groups: HSV expressing a constitutively active form of AKT (HSV-CA-AKT1), wild-type AKT (HSV-WT-AKT1) or β-galactosidase control (HSV-β-gal). AKT immunoreactive cells were counted in a blinded manner using three sections at 20x magnification per animal, which were averaged to obtain a mean count per animal, followed by averaging the mean counts of all animals within each treatment group. Data are presented as the mean ± SE number of AKT immunoreactive cells per treatment group. One-way ANOVA revealed significant differences in AKT-positive cell number between HSV-CA-AKT1, HSV-WT-AKT1, and HSV-β-gal control groups (F_{groups} (2,78) = 3.10, p = 0.05, one-way ANOVA). **, p < 0.01, as compared with HSV-β-gal-infused mice. Number of animals per group (n) are indicated. **(B)** Representative histology sections (4X; inset 20X) are shown for β-galactosidase (HSV-β-gal) treated mice to demonstrate the spread of the virus from the injection site within the nucleus accumbens. Lv = lateral ventricle, Ac = anterior commissure, Acb = nucleus accumbens. Insets, arrows point to β-galactosidase-immunoreactive neurons detected by anti-galactosidase antibody. **(C)** Basal locomotion in DBA/2J mice expressing HSV-delivered AKT1. DBA/2J mice were infused with HSV (bilateral striatum; 0.5µl/side infusion over 5 minutes; placement and expression verified by immunohistochemistry) expressing constitutively active form of AKT (HSV-CA-AKT1), wild-type AKT (HSV-WT-AKT1) or β-galactosidase (HSV-β-gal) 3 days prior to data collection. One-way ANOVA, $F_{treatment}(2,49) = 2.30$, p = 0.11. On the test day, mice were placed into a locomotor activity monitor and horizontal activity was quantified for 60 minutes. For all results, data are mean ± SEM. Number of animals per group (n) are indicated.

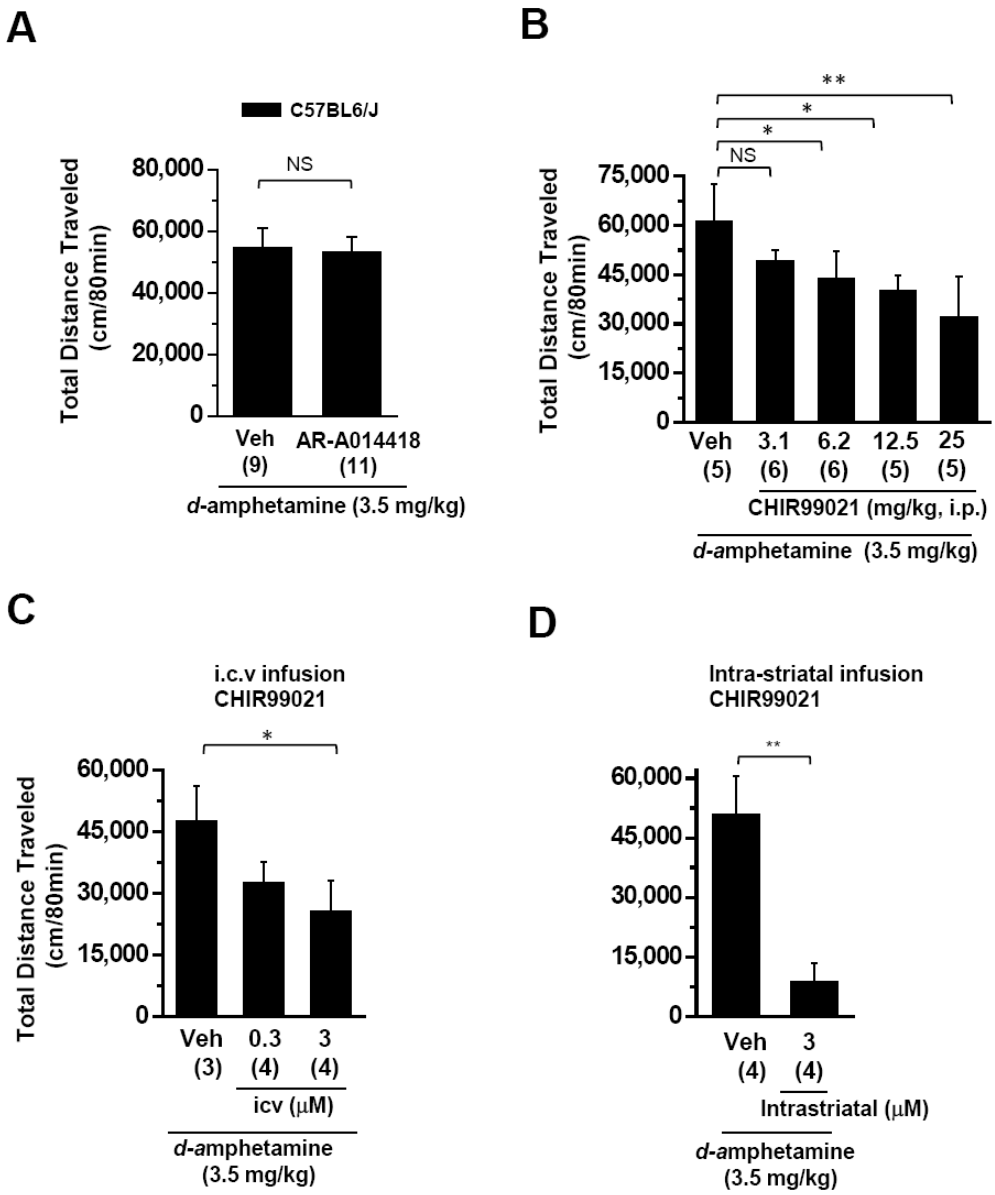

Supplemental Figure S6. Amphetamine-induced hyperlocomotion in the presence of AR-A014418 or CHIR99021. (A) C57BL/6J mice were treated with AR-A014418 (9 mg/kg, i.p.) or 100% DMSO (Veh) 60 minutes prior to amphetamine challenge (3.5 mg/kg, i.p.). Total activity was monitored for 80 minutes after the injection of *d*-amphetamine. Data are mean ± SEM. Number of animals per group (n) are indicated.

(B) C57BL/6J mice were treated with vehicle (45% PEG400, 45% saline, 10% DMSO) or CHIR99021 at different doses (25, 12.5, 6.1, 3 mg/kg i.p.) 60 minutes prior to *d*-amphetamine challenge (3.5 mg/kg, i.p.), and activity was monitored for 80 minutes after the *d*-amphetamine administration. One-way ANOVA, $F_{treatment}(4,22) = 3.34$, $p = 0.028$. **(C)** C57BL/6J mice were infused with CHIR99021 (Intracerebroventricular) at 0.3 and 3 μM and 60 minutes prior to amphetamine challenge (3.5 mg/kg, i.p.). Total activity was monitored for 80 minutes after the injection of *d*-amphetamine. One-way ANOVA, $F_{treatment}(2,10) = 5.42$, $p = 0.032$. **(D)** CHIR99021 was administrated intrastriatally to C57BL/6J mice one hour prior to amphetamine challenge (3.5 mg/kg, i.p.). Total activity was monitored for 80 minutes after the injection of *d*-amphetamine. One-way ANOVA, $F_{treatment}(1,6) = 28.9$, $p = 0.002$. **(E)** C57BL/6J mice were treated with different doses of CHIR99021 (25, 12.5, 6.1, 3 mg/kg i.p.) and baseline motor activity was monitored for 20 minutes prior to amphetamine administration. There were no differences between the groups in baseline motor activity after CHIR99021 administration $F_{treatment}(4,21) = 2.50$, $p > 0.05$. For all results, data are mean ± SEM. * $p < 0.05$, ** $p < 0.01$, *** $p < 0.0001$ as compared with vehicle-treated mice. Number of animals per group (n) are indicated.

Supplementary Table 1. Genotyping HT-22 cells. Genomic DNA from the HT-22 cell line was genotyped on a custom whole genome SNP (single nucleotide polymorphism) panel of 768 SNPs (unpublished) using Illumina GoldenGate technology at the Partners HealthCare Center for Personalized Genetic Medicine. HT-22 SNP genotypes were compared against data from 10 mouse inbred strains that are commonly used and reflect diverse branches of mouse strain phylogeny. HT-22 was found to be most similar to the FVB and SWR/J strains (87.9% and 82.3% identity across 768 SNPs, respectively), which are not responsive to lithium (Supplemental Material Figure S4; Gould et al. 2007).

Supplementary Table 2. KINOMEscan profiling of GSK-3β inhibitors. BIO, SB-216763, AR-A014418 and CHIR99021 were screened against 359 non-mutant kinases for competitive binding with active site binders using KINOMEscan technology. The complete list of kinases screened as well as competitive binding (% control) is shown.